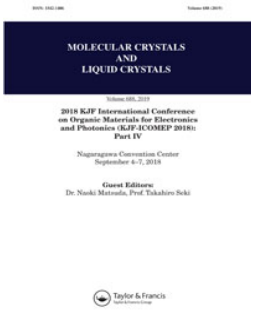

Molecular Crystals and Liquid Crystals

ISSN: 1542-1406 (Print) 1563-5287 (Online) Journal homepage: https://www.tandfonline.com/loi/gmcl20

Physical Properties in Thin Films of a Thienoimide End-capped Compound

H. Tachibana, N. Toda & R. Azumi

To cite this article: H. Tachibana, N. Toda & R. Azumi (2019) Physical Properties in Thin Films of a Thienoimide End-capped Compound, Molecular Crystals and Liquid Crystals, 688:1, 82-88, DOI: 10.1080/15421406.2019.1651072

To link to this article: https://doi.org/10.1080/15421406.2019.1651072

MOLECULAR CRYSTALS AND LIQUID CRYSTALS
2019, VOL. 688, NO. 1, 82–88
https://doi.org/10.1080/15421406.2019.1651072

Physical Properties in Thin Films of a Thienoimide End-capped Compound

H. Tachibana, N. Toda, and R. Azumi

National Institute of Advanced Industrial Science and Technology (AIST), Central 5, Higashi 1-1-1, Tsukuba 305-8565, Japan.

ABSTRACT

We have synthesized a new compound of a benzothiadiazole central core coupled to terminal thienoimide (TI) via vinyl linker, namely, C8-TI-BT. We investigated physical properties of vacuum-deposited and spin-coated thin films of C8-TI-BT. Optical properties of C8-TI-BT were different between thin films fabricated by vacuum deposition and spin-coating method. The vacuum-deposited films become more ordered structures by heat treatment. The thin-film transistor (TFT) shows ambipolar semiconducting behavior. We further demonstrated characteristics of electroluminescence (EL) device with the spin-coated C8-TI-BT films.

KEYWORDS
thienoimide; TFT; electroluminescence: heat treatment

1. Introduction

The design and synthesis of high-performance n-type organic semiconductors is one of the key factors for controlling various properties in electronic devices. Recently, insertion of phthalimide (PI) [1–3] and thienoimide (TI) [4–8] as a terminal acceptor unit has emerged as a powerful tool to obtain n-type small molecules. We have reported a photovoltaic performance of PI derivatives as n-type semiconductors [9].

In this work, we synthesized a new compound (C8-TI-BT) with terminal TI units bridged with central benzothiadiazole (BT) unit through vinyl linker units, and investigated its physical properties for vacuum deposited and spin-coated thin films of C8-TI-BT. We investigated thermal, optical, electrical, and optoelectronic properties evaluated by thin-film transistor (TFT) and electroluminescence (EL) devices and discuss the effect of fabrication methods of C8-TI-BT films.

2. Experimental

2.1. Synthesis

2.1.1. Synthesis of C8-TI-V

To a solution of bromo-thieno[3,2-c]pyrrole-4,6-dione 1 (4.72 g, 13.71 mmol), potassium vinyltrifluoroborate (2 g, 14.93 mmol), and K_2CO_3 (6.2 g, 44.86 mmol) in THF/H2O mixture (9:1; 100 ml), $Pd(PPh_3)_4$ (0.35 g, 0.30 mmol) was added. This mixture was heated to 85 °C for 24h. A crude product was purified by chromatography on silica gel

CONTACT H. Tachibana h-tachibana@aist.go.jp

(toluene). ^{1}H NMR (400 MHz, $CDCl_3$): δ 8.37 (d, $J = 16.0\,Hz$, 2H), 7.66 (s, 2H), 7.48 (d, $J = 16.0\,Hz$, 2H), 7.38 (s, 2H), 3.61 (t, 4H), 1.65 (m, 4H), 1.27-1.33 (m, 20H), 0.88 (m, 6H)

2.1.2. Synthesis of C8-TI-BT

To a solution of (2 g, 7.48 mmol), 1.4-dibromobenzodithiazole (0.73 g, 2.48 mmol), tetrabutylammonium bromide (1.6 g, 4.96 mmol), and CH_3COONa (0.61 g, 7.44 mmol) in DMF (50 ml), $Pd(OAc)_2$ (0.1 g, 13.41 mmol) was added under N_2 atmosphere. This mixture was heated at 100 °C for 48h. A crude product was purified by chromatography on silica gel ($CHCl_3$). ^{1}H NMR (400 MHz, $CDCl_3$): δ 8.37 (d, $J = 16.0\,Hz$, 2H), 7.66 (s, 2H), 7.48 (d, $J = 16.0\,Hz$, 2H), 7.38 (s, 2H), 3.61 (t, 4H), 1.65 (m, 4H), 1.27-1.33 (m, 20H), 0.88 (m, 6H). Anal. Calcd. For $C_{38}H_{42}N_4O_4S_3$: C, 63.84; H, 5.92; N, 7.84. Found: C, 63.87; H, 5.90; N, 7.77.

2.2. Film preparation

Solid thin films of C8-TI-BT were prepared by spin-coating chloroform solution and deposited by vacuum deposition onto glass plates for UV-visible absorption, AFM, and X-ray diffraction measurements. Heat treatments were carried out by heating the films for 10 minutes under ambient conditions. After the heat treatment, the thin films were cooled to room temperature prior to all the measurements.

2.3. Characterization

UV-visible absorption spectra of C8-TI-BT thin films were recorded using a JASCO V-780 spectrophotometer. Thermogravimetric (TGA) and differential scanning calorimetry (DSC) analysis was performed by using Seiko Instruments Inc. EXSTAR6000. Electrical measurements were performed using Keithley 4200-SCS semiconductor parametric analyzer in nitrogen atmosphere. X-ray diffraction (XRD) was acquired using Rigaku SmartLab with a monochromated Cu-Kα radiation. AFM measurements were performed using a SEIKO SPA300 microscope operating in a noncontact mode using a silicon tip with a resonance frequency of 28 kHz and a spring constant of 1.9 Nm^{-1}. Electroluminescence was measured using Keithley 2400 and Topcon BM-9 as luminance meter and source meter in air, respectively.

2.4. Device fabrication

For TFT measurement, the C8-TI-BT films were prepared on HMDS-treated substrates of p-type Si wafer with thermally grown SiO_2. The drain-source gold electrodes were evaporated through a shadow mask on top of the thin films. The channel length and the channel width were 20 μm and 2 mm, respectively.

For EL measurement, PEDOT-PSS aqueous solutions were spin-coating on ITO-coated glass substrate and the C8-TI-BT films were prepared on the ITO/PEDOT:PSS/glass. Al electrodes were evaporated on the C8-TI-BT films by vacuum deposition. The active area of the EL device was 4 mm^2.

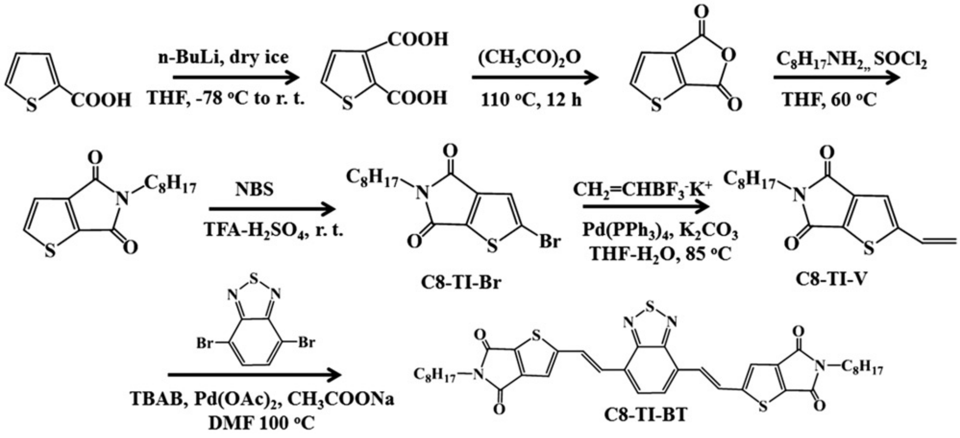

Scheme 1. Synthetic route for C8-TI-BT compound.

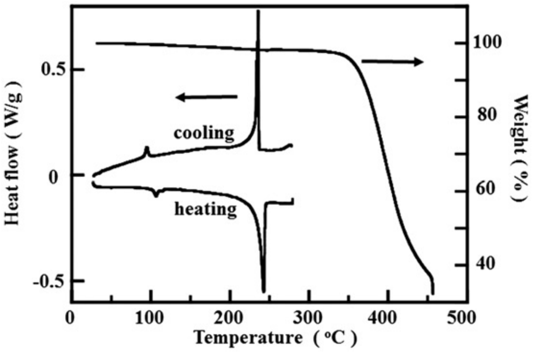

Figure 1. TGA and DSC thermograms of C8-TI-BT.

3. Results and Discussion

3.1. Synthesis

The synthetic routes for C8-TI-BT compound is shown in Scheme 1. C8-TI-Br was prepared according to methods described previously [6]. C8-TI-BT was synthesized with a slight modification of Suzuki-Heck coupling reactions [10,11]. The Suzuki reaction of C8-TI-Br and potassium vinyltrifluoroborate provide the vinyl-containing C8-TI and the Heck reaction of the resulting vinyl-containing C8-TI with 1,4-dibromobenzodithiazole yields C8-TI-BT. The structures of the obtained compounds were confirmed by NMR analysis.

3.2. Physical properties

The thermal behaviour of C8-TI-BT is analyzed by thermogravimetric analysis (TGA) and differential scanning calorimetry (DSC) under N_2 atmosphere as shown in Figure 1. The C8-TI-BT shows a good thermal stability with 5% weight loss at 355 °C. Heating DSC scans of C8-TI-BT are characterized by two endothermal peaks at 100 °C (4.2 J/g)

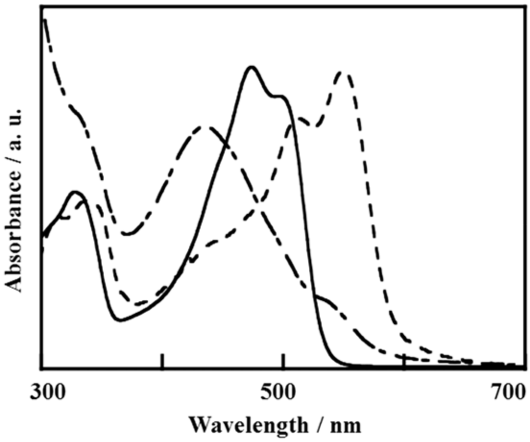

Figure 2. UV-visible absorption spectra for solution (solid line), spin-coated films (dotted line), and vacuum deposited films (dot-dashed line) of C8-TI-BT.

and 220 °C (50.9 J/g). Analysis of the temperature behavior of C8-TI-BT exhibit that the first transitions corresponds to crystal–crystal transformation due to alkyl chains, while the second one corresponds to the sample isotropization.

To compare the optical properties of vacuum-deposited and spin-coated films of C8-TI-BT, we measured UV-visible absorption spectra. Figure 2 shows UV-visible absorption spectra for both thin films. For comparison, an absorption spectrum in chloroform solution of C8-TI-BT is also plotted by solid lines. Although the absorption edge is almost the same for both vacuum-deposited and spin-coated films, the absorption peak and spectral profile are different. C8-TI-BT in solution has an absorption peak at 474 nm with a shoulder at 497 nm. C8-TI-BT for vacuum deposited films has a blue-shifted absorption peak at 435 nm with respect to that in solution. In contrast, C8-TI-BT shows a red-shifted absorption peak at 550 nm for spin-coated films. This is probably due to the difference in the molecular orientation of C8-TI-BT between the vacuum-deposited and spin-coated films. We investigated the change in UV-visible absorption spectra after heating thin films of C8-TI-BT at various temperatures for 10 min. The absorption peak and spectral profile of both vacuumed-deposited and spin-coated films after heating at 120 °C do not almost change compared with that before heating.

3.3. Vacuum deposition

Thin films of C8-TI-BT were deposited by vacuum deposition and used as active layer of TFT. We investigated the effect of heat treatment on the TFT device for C8-TI-BT thin films. Although TFT performance is not observed in the device before heating, the device after heating at 120 °C for 10 min shows ambipolar TFT characteristics. Figure 3(a) and 3(b) show transfer characteristics of C8-TI-BT measured at positive and negative source-drain bias after heat treatment at 120 °C, respectively. The device shows a n-type field-effect response with a mobility of 1.7 x10^{-6} cm^{2}V^{-1}s^{-1}. In contrast, the hole mobility was 1 order of magnitude lower than the electron mobility.

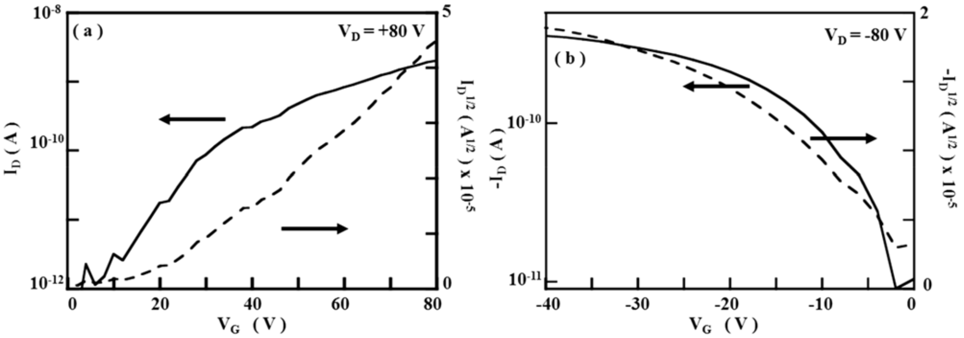

Figure 3. Transfer curves of a TFT device for vacuum deposited films of C8-TI-BT after heating at 120 °C.

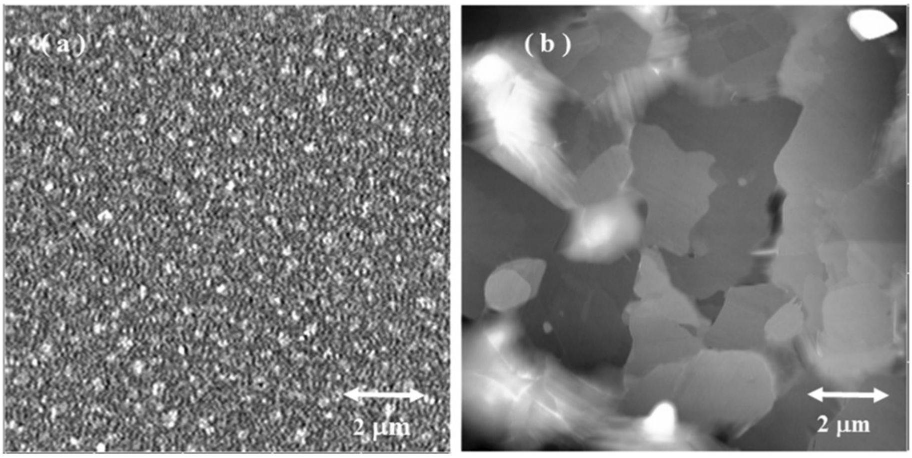

Figure 4. AFM images for vacuum deposited films of C8-TI-BT (a) before heating and (b) after heating at 120 °C for 10 min.

The morphological changes before and after heating were observed by AFM. Figure 4 shows the AFM images of the C8-TI-BT thin film before and after heating at 120 °C for 10 min. In the AFM image of before heating, the thin film surface is smooth with small domains. In contrast, the larger rounded and well-defined terraced grains are formed by heat treatment, which would facilitate the charge carrier transport. These behaviors are also supported by XRD measurements. Figure 5 shows the XRD patterns of C8-TI-BT films before and after heating at 120 °C. In the XRD patterns of the films before hating, the C8-TI-BT have no peaks other than broad peak at around 6° due to glass substrate. On the other hand, XRD pattern of the C8-TI-BT films after heating at 120 °C exhibits higher order periodicity of 3.08 nm, suggesting an almost perpendicular arrangement of the molecules respect to the substrate.

3.4. Solution deposition

Figure 6 shows the EL spectrum of the spin-coated C8-TI-BT film. For comparison, the photoluminescence (PL) is also plotted by dotted lines. The EL spectrum of C8-TI-BT

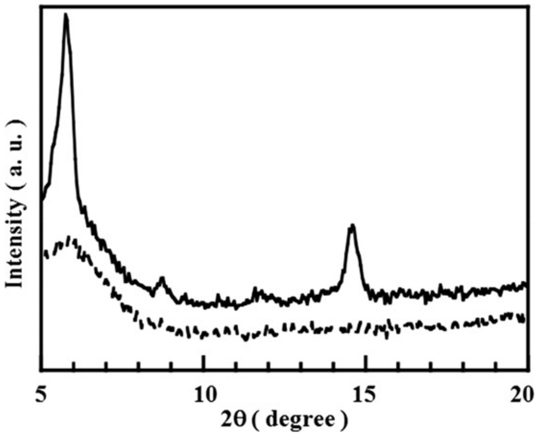

Figure 5. XRD patterns for vacuum deposited films of C8-TI-BT before heating (solid line) and after heating at 120 °C for 10 min (dotted line).

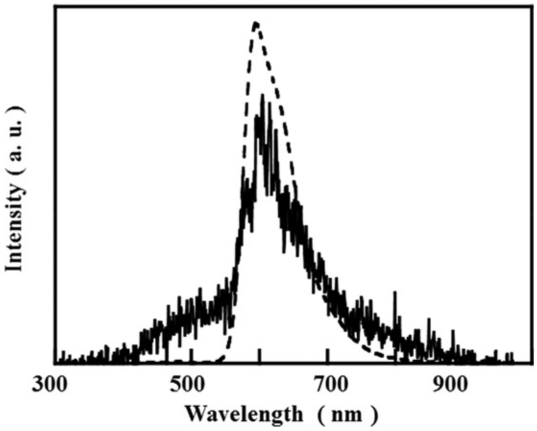

Figure 6. EL (solid line) and PL (dotted line) spectra for spin-coated films of C8-TI-BT.

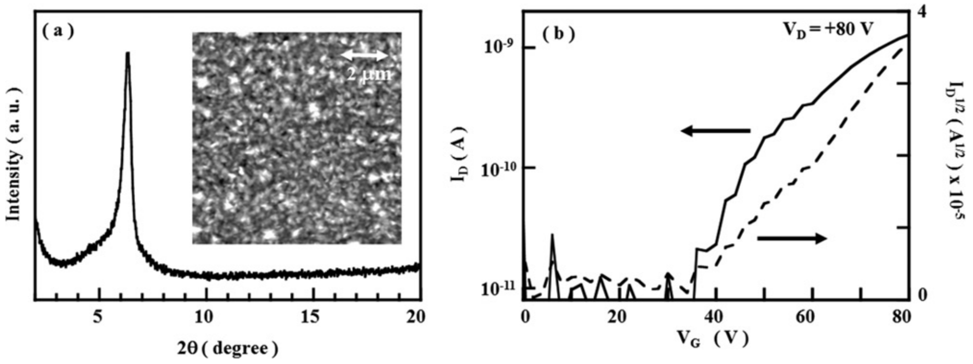

Figure 7. (a) XRD patterns, AFM images, and (b) transfer curves for spin-coated films of C8-TI-BT after heating at 120 °C.

was identical with that of PL in the films with the main EL and PL peaks at 600 nm, independence of heat treatment. The structures in C8-TI-BT films after heating at 120 °C were investigated by XRD and AFM measurements. As shown in Figure 7(a), the films exhibit small grains with lateral sized lower than 1 μm and shows the peak at 6.36° with the interlayer distance of 1.39 nm. The XRD patterns were identical with that of C8-TI-BT films before heating. The hole and electron mobility were the same order of magnitude as that for vacuum-deposited films (Figure 7(b)).

4. Conclusions

A new compound of a benzothiadiazole central core coupled to terminal thienoimide (TI) via vinyl linker, namely, C8-TI-BT was synthesized. We investigated physical properties of vacuum-deposited and spin-coated thin films of C8-TI-BT. Optical properties of C8-TI-BT were different between thin films fabricated by vacuum deposition and spin-coating method. The vacuum-deposited films become more ordered structures after heating at 120 °C. The thin-film transistor (TFT) shows ambipolar semiconducting behavior. We further investigated characteristics of electroluminescence (EL) device with the spin-coated C8-TI-BT films, in which the EL spectrum shows a peak at 600 nm.

References

[1] Bloling, J. T., Han, X., Higgs, A. T., Pastrop, J. P., Pandey, L., Norton, J. E., Risko, C., Chen, C. E., Breda, J-L., McGehhe, M. D., Sellinger., A. (2011). *Chem. Mater.*, *23*, 5484.

[2] Bloking, J. T., Giovenzana, T., Higgs, A. T., Ponec, A. J., Hoke, E. T., Vandewal, K., Ko, S., Bao, Z., Sellinger, A., McGehee., M. D. (2014). *Adv. Energy Mater.*, *4*, 1301426.

[3] O'Hara, K. A., Ostrowski, D. P., Koldemir, U., Takacs, C. J., Shaheen, S. E., Sellinger, A., Chabinyc., M. L. (2017). *ACS Appl. Mater. Interfaces*, *9*, 19021.

[4] Melucci, M., Zambianchi, M., Favaretto, L., Gazzano, M., Zanelli, A., Monari, M., Capelli, R., Troisi, S., Toffanin, S., Muccini., M. (2011). *Chem. Commun.*, *47*, 11840.

[5] Melcci, M., Durso, M., Bettini, C., Gazzano, M., Maini, L., Toffanin, S., Cavallini, S., Cavallin, M., Gentili, D., Biondo, V., Generali, G., Gallino, F., Capelli, R., Muccini., M. (2014). *J. Mater. Chem. C*, *2*, 3448.

[6] Douglas, J. D., Chen, M. S., Niskala, J. r., Lee, O. P., Yiu, A. T., Young, E. P., Frechet., J. M. J. (2014). *Adv. Mater.*, *26*, 4314.

[7] Benvenuti, E., Gentili, D., Chiarella, F., Portone, A., Barra, M., Cecchini, M., Cappuccino, C., Zambianchi, M., Lopez, S. G., Salzillo, T., Venuti., E. Cassinese, A., Pisignano, D., Persano, L., Cavallini, M., Mairi, L., Melucci, M., Muccini, M., Toffanin., S. (2018). *J. Mater. Chem. C*, *6*, 5601.

[8] Cappuccion., C. Mazzeo, P. P., Salzillo, T., Venuti, E., Giunchi, A., Valle, R. G. D., Brillante, A., Bettini, C., Melucci, M., Maini., L. (2018). *Phys. Chem. Chem. Phys.*, *20*, 3630.

[9] Mochizuki, H., Tachibana, H., International Conference on Solid State Device and Materials 2017 (SSDM 2017), Fukuoka, Japan, September, Abstr. No. PS-10-05, (2017).

[10] Molander, G. A., Brown., A. R. (2006). *J. Org. Chem.*, *71*, 9681.

[11] Alacid, E., Najera., C. (2008). *Adv. Synth. Catal.*, *350*, 1316.